







A high-performance asymmetric supercapacitor consists of binder free electrode materials of bimetallic hydrogen phosphate ($\text{MnCo}(\text{HPO}_4)$) hexagonal tubes and graphene ink

Kwang-Seon Ahn^a, Rajangam Vinodh^{b,c}  , Bruno G. Pollet^c, Rajendran Suresh Babu^d, Vanaraj Ramkumar^e, Seong-Cheol Kim^e, Kungumaraj Krishnakumar^f, Hee-Je Kim^a  

[Show more](#) 

 Share  Cite

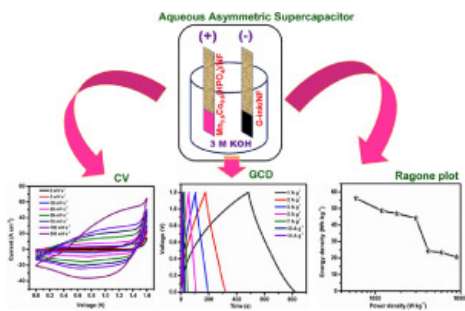
<https://doi.org/10.1016/j.electacta.2022.140763> 

[Get rights and content](#) 

Abstract

Novel bimetallic manganese-cobalt hydrogen phosphate ($\text{Mn}_x\text{Co}_x(\text{HPO}_4)$) hexagonal tubes were efficiently prepared by a direct and simple chemical bath deposition (CBD) procedure. The prepared $\text{Mn}_x\text{Co}_x(\text{HPO}_4)$ materials have been analysed through Fourier transform infrared (FT-IR), thermogravimetric analysis (TGA), and X-ray diffraction (XRD) methods. The surface morphology and the particle size of the materials were studied using field emission scanning electron microscopy (FE-SEM) and high-resolution transmission electron microscopy (HR-TEM). The textural characteristics and elemental composition of the $\text{Mn}_x\text{Co}_x(\text{HPO}_4)$ were measured using nitrogen sorption isotherms and X-ray photoelectron spectroscopy (XPS) analysis. Owing to its unique hexagonal structures and porous nature, the $\text{Mn}_{0.5}\text{Co}_{0.5}(\text{HPO}_4)$ electrode is measured *via* a three-electrode system and achieved the highest specific capacitance of $1,727 \text{ F g}^{-1}$ at the current density of 1.0 A g^{-1} . An aqueous asymmetric supercapacitor (AAS), $\text{Mn}_{0.5}\text{Co}_{0.5}(\text{HPO}_4)//\text{G-ink}$ device based on $\text{Mn}_{0.5}\text{Co}_{0.5}(\text{HPO}_4)$ as the cathode and graphene ink (G-ink) as an anode material. The fabricated device might function well in a large operating potential window of $+1.6 \text{ V}$. The $\text{Mn}_{0.5}\text{Co}_{0.5}(\text{HPO}_4)//\text{G-ink}$ AAS exhibited the maximum power and specific energy of $9,000 \text{ W kg}^{-1}$ and 56.16 Wh kg^{-1} , correspondingly at 1.0 A g^{-1} . Furthermore, the fabricated device could withstand 95.5% of its primary capacitance after 5,000 galvanostatic charge/discharge (GCD) turns, which illustrates that the materials could be a prominent contender for supercapacitor applications.

Graphical abstract



[Download : Download high-res image \(211KB\)](#)

[Download : Download full-size image](#)

Introduction

In the present scenario, the rapid consumption of fossil fuels and the associated crucial environmental problems have forced scientists and engineers to find environment-friendly, less-cost, effective, and sustainable energy storage, and conversion technologies [1], [2]. Supercapacitors (SCs) are promising in a variety of areas, including telecommunications equipment, pulse laser technique, digital cameras, smartphones, power utensils, electric hybrid vehicles, uninterruptible electric supply to computers/laptops, and energy storage created by solar cells [3, 4]. Capable of existing with other electrochemical devices such as batteries, the specific energy of the SCs must be significantly boosted with the specific power and cyclic stability [5]. The specific energy (E_d) improves with the specific capacitance of the device (C_s) and the operating potential window (V) rendering to the following equation $E=0.5 C_s \times V^2$ [6].

In recent years, metal phosphate ($M-(PO_3)^{2-}$) related electrode materials have drawn much interest due to their extreme electrochemical activity and layered architecture assembly [7, 8]. The two crucial factors, such as excellent chemical stability and superior conductivity are the primary criteria for any electrode resources in SCs or Li-ion batteries (LIB) [9]. In the solid form of open framework, $M-(PO_3)^{2-}$ have large networks and pores that can produce high ionic and charge densities when employed as pseudocapacitive electrode materials [10]. Furthermore, the oxyanion of pentavalent phosphorus can prime to various phases of $M-(PO_3)^{2-}$ [11]. Different types of valance states through surface reactions can increase the conductivity of $M-(PO_3)^{2-}$ electrodes [12]. Metal hydrogen phosphate (MHP; $M-HPO_4$) is the part of $M-(PO_3)^{2-}$ the family that has fascinating, layered surface/interface structures which are effortlessly available to ions in the electrolyte and have virtuous intercalation of ions in energy storage applications [13]. As far as we know, there are very few papers reported in $M-HPO_4$ electrode materials for supercapacitors. For instance, Huan Pang et al. [14] prepared $CoHPO_4 \cdot 3H_2O$ nanosheets by a simplistic hydrothermal technique for SC applications. The synthesized $CoHPO_4 \cdot 3H_2O$ was performed well in a 3-electrode cell and exposed the highest specific capacitance ($413 F g^{-1}$). Of late, Abdulmajid A. Mirghni et al. [15] have produced $NaNi_4(PO_4)_3/GF$ composite *via* precipitation method and it displayed a maximum of $63.3 mAh g^{-1}$ at $1.0 A g^{-1}$ specific capacity in a three-electrode configuration. In addition, the constructed $NaNi_4(PO_4)_3/GF//AC$ ASC revealed the high specific power with the specific energy of $570 W kg^{-1}$ and $19.5 Wh kg^{-1}$, correspondingly at $0.5 A g^{-1}$. Yufeng Zhao et al. [16] described ammonium cobalt-nickel phosphates electrode material consisting of $(Ni, Co)_3(PO_4)_2 \cdot 8H_2O$ and $(NH_4)(Ni, Co)PO_4 \cdot 0.67H_2O$ by hydrothermal method. The composite material delivers a maximum capacitance of $1,128 F g^{-1}$ at $0.5 A g^{-1}$. Furthermore, the fabricated ASC delivered a high specific power and specific energy of $4,400 W kg^{-1}$ and $35.3 Wh kg^{-1}$ accompanied with outstanding cyclic stability (95.6% of capacitance retention after 5,000 galvanostatic charge/discharge - GCD cycles). Zhang et al. [17] stated that core-shell $Co_{11}(HPO_3)_8(OH)_6-Co_3O_4$ hybrids for supercapacitor electrode material with a maximum capacitance of $1.84 mF cm^{-2}$ at $0.5 mA cm^{-2}$. In addition, the fabricated asymmetric device exhibited the highest power densities of $105 mW cm^{-3}$ at $1.5 mA cm^{-2}$. Yang et al. [18] synthesized $Mn_3(PO_4)_2 \cdot 3H_2O$ NSs/G (manganese phosphate nanosheets/graphene) composites for SCs studies. The assembled ASC exhibited a supreme specific capacitance of $152 F g^{-1}$ at $0.5 A g^{-1}$ along with specific energy ($0.17 \mu Wh cm^{-2}$ at $0.5 A g^{-1}$) and specific power ($46 \mu W cm^{-2}$ at $2.0 A g^{-1}$). Furthermore, ASC displayed an exceptional cyclic steadiness and almost cent percent capacitance maintenance was achieved over 2,000 GCD cycles. Recently, Wang et al. [19] prepared cobalt-nickel phosphate composite for ASC applications. The ASC device presented the highest capacitance of $298.65 F g^{-1}$ at $1 A g^{-1}$ and could reach specific energy of $19.31 Wh kg^{-1}$ at a specific power of $163.42 W kg^{-1}$. Liu et al. [20] synthesized

$\text{Ni}_3\text{P}_2\text{O}_8\text{-Co}_3\text{P}_2\text{O}_8\text{-8H}_2\text{O}$ by a superficial chemical precipitation technique and it displayed the extreme capacitance of $1,974 \text{ F g}^{-1}$ at 0.5 A g^{-1} .

Nevertheless, the aforementioned approaches require several complicated steps, such as the need for expensive equipment (high-pressure autoclave) for hydrothermal method consuming urea (COH_4N_2)/ammonium hydroxide (NH_4OH) as a reducing agent. Depending on the template method, removing the hard template, or selecting/embedding it in the appropriate solvent causes the final material impure and time-consuming. Though, in this current investigation, a simple chemical bath deposition (CBD) method was employed to yield $\text{Mn}_x\text{Co}_x(\text{HPO}_4)$ with good hexagonal tube morphology. CBD requires only a glass bottle with a lid and hot-air oven. In addition, the present synthesis method requires source materials of Mn, Co, and hydrogen phosphate with distilled water. Additionally, no reports are available to date for the preparation of (HPO_4) hexagonal tubes for supercapacitor applications.

Transition metal oxides (TMOs), such as iron oxides (Fe_2O_3), manganese oxides (MnO_2), cobalt oxides (CoO), nickel oxides (NiO), and are extensively studied as electrode materials for supercapacitor applications owing to their noble electrochemical outcome. However, the TMOs suffer inferior rate capability and poor cyclic performance of the electrode materials. To overcome these issues, manganese cobalt phosphates are considered a potential choice due to their cheap prices, lesser harmfulness, facile preparation method, and high theoretical specific capacity [21, 22]. In addition, generally HPO_4 ion exhibit three distinct pK_a values of 2.16 (H_2PO_4^-), 7.21 (HPO_4^{2-}), and 12.67 (PO_4^{3-}). With a greater pK_a value and sturdier nucleophilic ability, the above values govern their nucleophilic capability. So, MHPs may deliver an additional effective proton pair electron transfer method than metal phosphates [23, 24].

Herein, we provide a straightforward method to prepare a hexagonal tube of $\text{Mn}_x\text{Co}_x(\text{HPO}_4)$ in a chemical bath deposition procedure by applying $\text{MnSO}_4\cdot\text{H}_2\text{O}$ and $\text{Co}(\text{NO}_3)_2\cdot 6\text{H}_2\text{O}$ precursors. In addition, we examined the electrochemical evaluation of the *as*-prepared materials *via* a traditional three-electrode configuration, and the $\text{Mn}_{0.5}\text{Co}_{0.5}(\text{HPO}_4)$ hexagonal tubes showed the superior electrochemical performance for energy storage. More importantly, the construction of an AAS device composed of the hexagonal tube structured manganese-cobalt hydrogen phosphate ($\text{Mn}_{0.5}\text{Co}_{0.5}(\text{HPO}_4)$) as a positive electrode and G-ink as a negative electrode in 3.0 M KOH as the supporting electrolyte. The constructed AAS device shows a supreme specific capacitance of 280.8 F g^{-1} at 1.0 A g^{-1} . The AAS demonstrated a high specific energy of 56.16 Wh kg^{-1} at a specific power of 599.92 W kg^{-1} . Furthermore, the assembled AAS shows a slight capacitance change after 5,000 charge/discharge cycles at 5.0 A g^{-1} (95.5% capacitance retention).

Section snippets

Materials

$\text{Mn}(\text{NO}_3)_2\cdot 6\text{H}_2\text{O}$ (99% of Manganese (II) nitrate hexahydrate) and $\text{Co}(\text{NO}_3)_2\cdot 6\text{H}_2\text{O}$ (99% of cobalt (II) nitrate hexahydrate) was procured from Daejung Chemicals, South Korea. Na_2HPO_4 (99% of sodium phosphate dibasic) was obtained from Sigma-Aldrich, USA. NF (nickel foam) was acquired from Sigma-Aldrich for electrode fabrication....

Preparation of $\text{Mn}_x\text{Co}_x(\text{HPO}_4)$

$\text{Mn}_{0.25}\text{Co}_{0.75}(\text{HPO}_4)$ was prepared by a facile and efficient CBD method. In brief, the required amounts of $\text{Mn}(\text{NO}_3)_2\cdot 6\text{H}_2\text{O}$ (1.10 g), $\text{Co}(\text{NO}_3)_2\cdot 6\text{H}_2\text{O}$ (1.89 g), and deionized water (100...

Physicochemical characterizations of $\text{Mn}_x\text{Co}_x(\text{HPO}_4)$

The surface morphology of electrode materials derived for supercapacitor application is crucial because all electrochemical reactions take place on or close to the electrode surface, and distinct morphology has diverse ion transfer rates and electrode/electrolyte interface properties [25]. Hence, the morphology of the $\text{Mn}_x\text{Co}_x(\text{HPO}_4)$ governs its electrochemical properties. The surface morphology of the prepared materials was studied by SEM and TEM analysis. The SEM pictures (Fig. 1(a) - 1(c2))...

Conclusions

In summary, bimetallic hydrogen phosphate ($\text{Mn}_x\text{Co}_x(\text{HPO}_4)$) materials have been successfully prepared by the CBD method for electrochemical energy storage devices. The hexagonal tube-like morphology was established by SEM and TEM methods. The maximum surface area of $132 \text{ m}^2 \text{ g}^{-1}$ was achieved for $\text{Mn}_{0.5}\text{Co}_{0.5}(\text{HPO}_4)$. The maximum specific capacitance of 1,177, 1727, and 449 F g^{-1} was obtained for $\text{Mn}_{0.25}\text{Co}_{0.75}(\text{HPO}_4)$, $\text{Mn}_{0.5}\text{Co}_{0.5}(\text{HPO}_4)$, and $\text{Mn}_{0.75}\text{Co}_{0.25}(\text{HPO}_4)$, respectively at a specific current of 1.0 A g^{-1} ...

CRedit authorship contribution statement

Kwang-Seon Ahn: Data curation, Writing – original draft. **Rajangam Vinodh:** Data curation, Writing – original draft. **Bruno G. Pollet:** Supervision, Visualization, Investigation. **Rajendran Suresh Babu:** Conceptualization, Methodology. **Vanaraj Ramkumar:** Conceptualization, Methodology. **Seong-Cheol Kim:** Software, Validation, Writing – review & editing. **Kungumaraj Krishnakumar:** Software, Validation, Writing – review & editing. **Hee-Je Kim:** Supervision, Visualization, Investigation....

Declaration of Competing Interest

The authors declare that they have no known competing financial interests or personal relationships that could have appeared to influence the work reported in this paper....

Acknowledgment

This research work was supported by BK21 Plus Creative Human Resource Education and Research Programs for ICT Convergence in the 4th Industrial Revolution, Pusan National University, Busan, South Korea....

[Recommended articles](#)

References (57)

J. Niu *et al.*

[Requirements for performance characterization of C double-layer supercapacitors: applications to a high specific-area C-cloth material](#)

J. Power Sources (2006)

Y. Zhang *et al.*

[Core-shell \$\text{Co}_{11}\(\text{HPO}_3\)_8\(\text{OH}\)_6\text{-Co}_3\text{O}_4\$ hybrids for high-performance flexible all-solid-state asymmetric supercapacitors](#)

J. Alloys Compd. (2015)

M.-C. Liu *et al.*

[Design and fabrication of \$\text{Ni}_3\text{P}_2\text{O}_8\text{-Co}_3\text{P}_2\text{O}_8\cdot 8\text{H}_2\text{O}\$ as advanced positive electrodes for asymmetric supercapacitors](#)

Electrochim. Acta (2016)

J. Yang *et al.*

[Nickel phosphate molecular sieve as electrochemical capacitors material](#)

J. Power Source (2014)

J. Gomez *et al.*

[High-performance binder-free Co–Mn composite oxide supercapacitor electrode](#)

J. Power Source. (2013)

A.N. Naveen *et al.*

Investigation on physiochemical properties of Mn substituted spinel cobalt oxide for supercapacitor applications

Electrochim. Acta (2014)

J.L. Gautier *et al.*

Characterisation by X-ray photoelectron spectroscopy of thin $\text{Mn}_x\text{Co}_{3-x}\text{O}_4$ ($1 \geq x \geq 0$) spinel films prepared by low-temperature spray pyrolysis

Thin Solid Film. (1997)

A.D. Jagadale *et al.*

Performance evaluation of symmetric supercapacitor based on cobalt hydroxide $[\text{Co}(\text{OH})_2]$ thin-film electrodes

Electrochim. Acta (2013)

S. He *et al.*

3D porous and ultralight carbon hybrid nanostructure fabricated from carbon foam covered by monolayer of nitrogen-doped carbon nanotubes for high performance supercapacitors

J. Power Source. (2015)

X. Li *et al.*

Fabrication of $\gamma\text{-MnS/rGO}$ composite by facile one-pot solvothermal approach for supercapacitor applications

J. Power Source. (2015)



View more references

Cited by (25)

Hierarchical nanoassembly of $\text{Ni}_3\text{S}_2\text{-MoS}_2$ interconnected with CeO_2 as a highly remarkable hybrid electrocatalyst for enhancing water oxidation and energy storage

2024, Journal of Energy Storage

Show abstract

Advancements in asymmetric supercapacitors: Material selection, mechanisms, and breakthroughs with metallic oxides, sulfides, and phosphates

2023, Journal of Energy Storage

Show abstract

Transition metal phosphates: A paradigm for electrochemical supercapacitors

2023, Journal of Electroanalytical Chemistry

Show abstract

Synthesis of MoS_2/CoS composite electrode and its application for supercapacitors

2023, Journal of Alloys and Compounds

Show abstract

NiCoP/Co₉S₈ nanoflowers as advanced electrode material for asymmetric supercapacitors

2023, Journal of Alloys and Compounds

[Show abstract](#) 

Recent progress on phosphate-based electroactive materials for supercapacitor applications

2023, Results in Surfaces and Interfaces

[Show abstract](#) 



[View all citing articles on Scopus](#) 

[View full text](#)

© 2022 Elsevier Ltd. All rights reserved.



All content on this site: Copyright © 2024 Elsevier B.V., its licensors, and contributors. All rights are reserved, including those for text and data mining, AI training, and similar technologies. For all open access content, the Creative Commons licensing terms apply.

